SUPPLEMENTARY INFORMATION

A Conserved Allosteric Pathway in Tyrosine Kinase Regulation

William M. Marsiglia[1], Joseph Katigbak[1‡], Sijin Zheng[1‡], Moosa Mohammadi[2], Yingkai Zhang[1,3], and Nathaniel J. Traaseth[1]*

[1] Department of Chemistry, New York University, New York, NY 10003, USA

[2] Department of Biochemistry & Molecular Pharmacology, New York University School of Medicine, New York, NY 10016, USA

[3] NYU-ECNU Center for Computational Chemistry at NYU Shanghai, Shanghai 200062, China

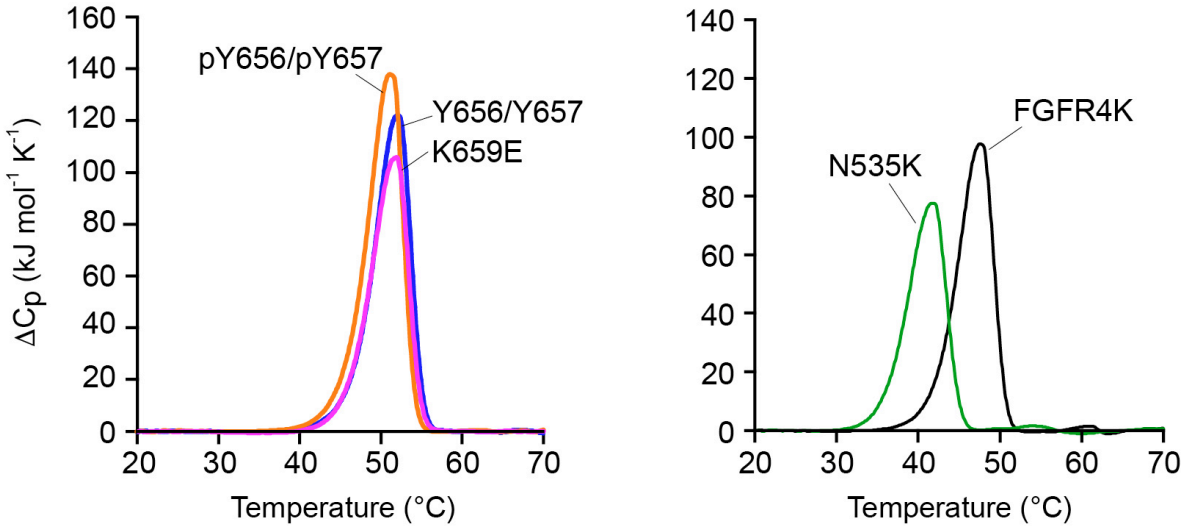

Figure S1. Supplemental figure related to Figure 1. Differential scanning calorimetry (DSC) thermograms showing that molecular brake mutants have a destabilizing effect relative to wild-type FGFRK, whereas A-loop mutation/phosphorylation do not change the melting temperature. (Left) Thermogram data measured using DSC comparing unphosphorylated FGFR2K (blue; Y656/Y657), A-loop phosphorylated FGFR2K (orange; pY656/pY657), and the most pathogenic A-loop mutant K659E of FGFR2K (magenta; K659E). Note that to ensure a well-defined phosphorylated state (i.e., phosphorylation at Y656 and Y657), the Y656/Y657 and pY656/Y657 samples had mutations at other tyrosine residues (Y466, Y586L, Y588S). (Right) Thermogram data measured using DSC for wild-type FGFR4K (black; FGFR4K) and an FGFR4K molecular brake mutant (green; N535K) corresponding to the N549K mutation in FGFR2K.

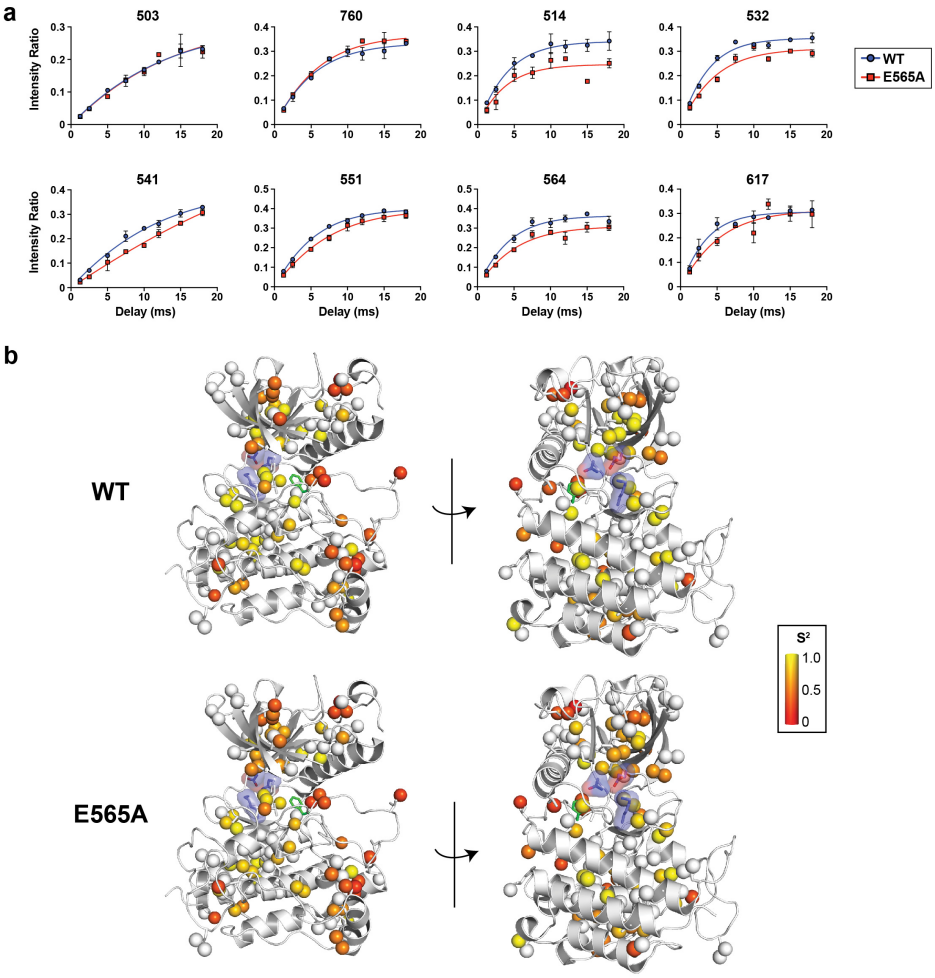

Figure S2. Supplemental figure related to Figure 2. (a) Representative NMR fitted curves of ^{1}H-^{1}H dipolar cross-correlated relaxation rate (η) experiments used to derive order parameters (S^2). Example overlays of intensity ratio curves calculated as the intensity of triple quantum (forbidden) peaks divided by single quantum intensities as a function of the mixing delay. Wild-type FGFR2K data are shown in blue circles, while the E565A mutant from FGFR2K are shown in red squares. Example curves displayed for residues I503 (in the β2-β3 loop) and I760 (in the αI helix) showed no difference in η (s^{-1}) values between wild-type FGFR2K and E565A. The other plots corresponding to residues 514, 532, 541, 551, 564, and 617 displayed different η (s^{-1}) values between wild-type FGFR2K and E565A. Error bars represent the standard deviation of the intensity ratio from duplicate measurements. Fitted η (s^{-1}) values and corresponding errors for all residues are listed in Table S2. (b) Experimentally derived order parameters (S^2) plotted on a cartoon representation of FGFR1K (PDB ID: 3KY2). The top panels display S^2 values for wild-type FGFR2K, while the bottom panels show S^2 values for the molecular brake E565A mutation of FGFR2K. Two structural views are displayed for each dataset. Spheres depict Ile, Val, and Leu methyl sites used for the NMR measurements. White spheres indicated methyl sites that could not be assigned or sites that could not be analyzed due to spectral overlap. The remaining spheres are colored according to the scale: red, $S^2 = 0$; yellow, $S^2 = 1$. The phenylalanine displayed in green is F645 from the DFG motif, while the residues in the blue surface correspond to the molecular brake residues of FGFR2K: N549, E565, and K641.

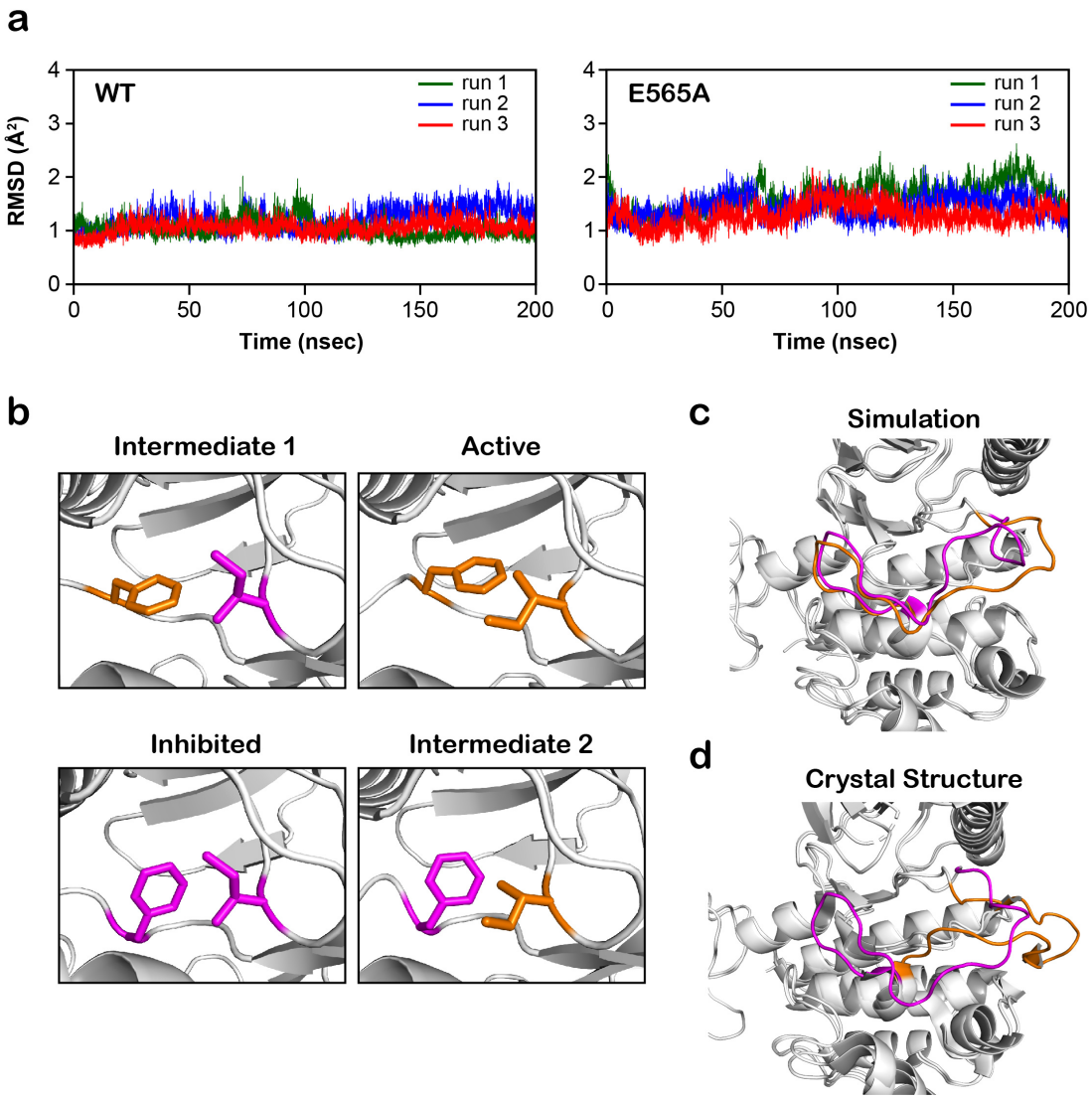

Figure S3. Supplemental figure related to Figure 3. (a) The RMSD time series of molecular dynamics simulations run on wild-type FGFR1K and the single site E565A mutant. Each of the three replica 200 nsec simulations are shown in a different color: run 1, green; run 2, blue; run 3, red. The plot on the left displays wild-type FGFR1K, while the plot on the right displays the E565A results. RMSD values were calculated using heavy atoms (CA, C', N, and O) of the kinase domain that excluded the A-loop and kinase insert regions. (b) Representative structural views from molecular dynamics simulations highlighting residues I547 and F645 (i.e., Phe from DFG motif). The four rotamer combinations correspond to those displayed in Figure 3b and 3c. The inhibited-like rotamers are shown in magenta and the active-like rotamers are shown in orange. (c) Superimposition of representative structures from molecular dynamics simulations highlighting the A-loop conformations. The magenta A-loop corresponds to inhibited rotamers of I547 and F645 as depicted in panel (b), while the orange A-loop has active-like rotamers for I547 and F645. (d) Superimposition of inhibited (PDB ID: 3KY2) and active crystal structures (PDB ID: 2PVF) with the A-loops of the kinase highlighted in magenta (inhibited) and orange (active) colors.

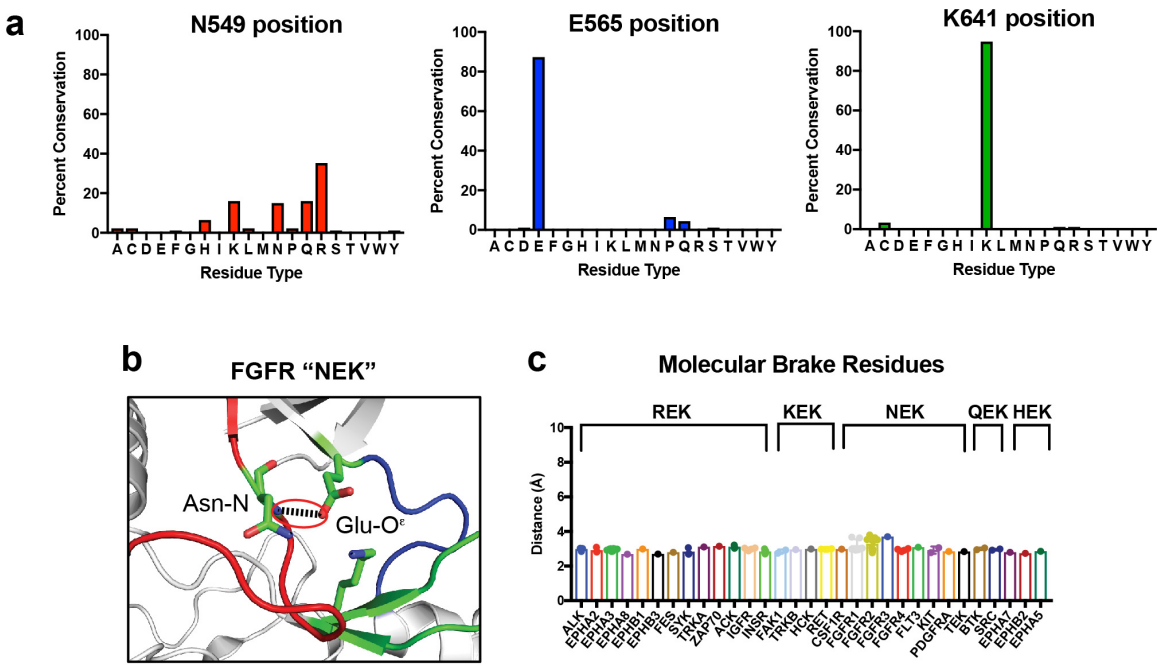

Figure S4. Supplemental figure related to Figure 4. (a) The molecular brake residues glutamic acid and lysine are highly conserved in tyrosine kinases. Homology modeling results of all tyrosine kinases at the three molecular brake residues displayed as the conservation of the position (normalized to 100%) as a function of the 20 amino acid residues. The molecular brake residues of N549 (left, red), E565 (center, blue), and K641 (right; green) correspond to the numbering convention of FGFR2K. (b) Structural view of the molecular brake for FGFR1K (PDB ID: 3KY2) depicting the interaction between the side chain oxygen of the glutamic acid (E565 in FGFR2K numbering) with the backbone nitrogen from the asparagine position (N549 in FGFR2K numbering). The kinase molecule is shown as a gray cartoon; αC-β4 loop, kinase hinge, and β8 strand contributing residues to the molecular brake are highlighted in red, blue and green, respectively. The triad of residues (i.e., N549, E565 and K641) comprising the molecular brake are shown as green sticks. Oxygen and nitrogen atoms are colored red and blue, respectively; the hydrogen bond between E565 and N549 is denoted by a dashed black line. (c) Conservation of hydrogen bonding at the molecular brake for tyrosine kinases that do not share the asparagine position of the molecular brake present within the FGFR subfamily. Measured distances for available tyrosine kinase structures within the PDB corresponding to the backbone nitrogen of the analogous N549 position (FGFR2K numbering) with the side chain oxygen of the analogous E565 (FGFR2K numbering). Note that only kinases sharing the glutamic acid and lysine positions within the molecular brake were analyzed. The three letter titles above the brackets depict the three residues comprising the molecular brake. For example, kinases with asparagine, glutamic acid, and lysine are labeled "NEK" and are shared in FGFR, VEGFR, PDGFR, c-KIT, TIE, TEK, CSF1R, and FLT3.

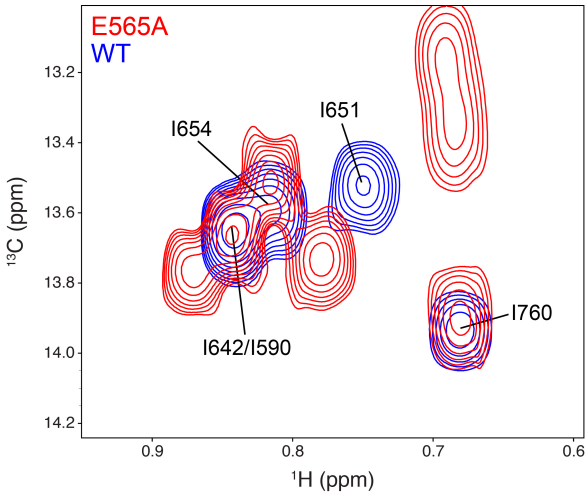

Figure S5. Supplemental figure related to Figure 2. Mutation at the molecular brake perturbs chemical shifts corresponding residues within the A-loop. $^{1}H/^{13}C$ HMQC spectra of ILV labeled wild-type FGFR2K (blue spectra) and the single site mutation E565A of FGFR2K (red spectra). The spectral overlay highlights that A-loop residues such as I651 and I654 are perturbed between wild-type FGFR2K and the molecular brake mutant. Both HMQC datasets were acquired at 10 °C and the concentration of each kinase was 0.5 mM.

Table S1. Supplemental table related to Figure 1. Mutations in cancers that occur in one of the three molecular brake residues of tyrosine kinases. Data were obtained from the Catalogue of Somatic Mutations in Cancer (COSMIC) database: https://cancer.sanger.ac.uk/cosmic.

Kinase	Molecular Brake[a]	N549 position	E565 position	K641 position
EGFR	RQK	C/H/S/L/G		N/R
ErbB2	RQK	K/H	P	
ErbB4	RQK	Q		
EphA3	REK	Q	K	N/M
EphA6	REK			N
EphB1	REK	C/H		
EphB3	REK	W	Q	
EphB4	REK	C		
EphA8	REK	H		
EphA2	REK	L/C		
LYN	REK	S	Q	
BLK	REK	Q		
FES	REK	H		
IGF1R	REK			R
EphA5	HEK		Q/V	
EphA7	HEK	N		
EphB2	HEK		K	R
DDR2	HEK			N
JAK2	KEK	T		
JAK3	KEK	E		
MUSK	KEK		D	
HCK	KEK		K	
RET	KEK	N/E		
ABL	QEK			R
SRC	QEK		K	
FGFR2	NEK	S/D/K/H	K/G/A	R
FGFR3	NEK	S		
FGFR1	NEK	K/D		
FGFR4	NEK	K		
KDR	NEK	S		
KIT	NEK	K		N/R
PDGFRa	NEK	K/Y/S/D/H	Q	
PDGFRb	NEK	S		
FLT3	NEK	K/T		
TIE1	NEK		G	
AXL	RPC	K	L	
MET	SPK	W		
DDR1	RDK	W/L		
ROR1	CEK			N
ROR2	CSK			N

[a] The three molecular brake positions of N549, E565, and K641 correspond to the numbering of FGFR2K and are denoted as "NEK" under the "Molecular Brake" heading.

Table S2. Supplemental table related to Figure 2 that lists NMR derived order parameters (S^2) and η values for wild-type FGFR2K (top) and E565A (bottom). Errors reflect non-linear least square fitting errors from datasets acquired in duplicate.

	Residue	η (s^{-1})	Error η (s^{-1})	S^2	Error S^2
	I503	31.30	1.76	0.32	0.02
	I541	43.45	2.12	0.45	0.02
	I547	90.54	9.48	0.93	0.10
	I548	99.12	5.97	1.02	0.06
	I563	77.46	9.01	0.80	0.09
	I590	37.89	0.82	0.39	0.01
	I623	55.14	2.79	0.57	0.03
	I651	27.68	1.48	0.28	0.02
	I654	40.29	0.92	0.41	0.01
	I696	89.81	6.15	0.92	0.06
	I707	30.11	0.87	0.31	0.01
	I760	76.85	5.61	0.79	0.06
	V463	12.16	0.33	0.12	0.00
	V495	83.37	4.11	0.86	0.04
	V496	36.95	0.97	0.38	0.01
	V512	72.72	3.88	0.75	0.04
	V514	104.10	8.29	1.07	0.09
	V514	102.30	10.63	1.05	0.11
	V516	96.38	5.29	0.99	0.05
	V516	92.10	3.98	0.95	0.04
	V532	117.80	7.10	1.21	0.07
	V532	94.92	3.38	0.97	0.03
	V562	107.10	3.38	1.10	0.03
wild-type	V564	102.30	4.30	1.05	0.04
	V564	106.20	7.97	1.09	0.08
	V593	55.21	2.32	0.57	0.02
	V593	39.81	1.56	0.41	0.02
	V634	95.61	5.71	0.98	0.06
	V634	101.80	9.39	1.05	0.10
	V639	92.51	7.08	0.95	0.07
	V667	91.44	4.83	0.94	0.05
	V679	67.13	2.90	0.69	0.03
	V691	91.93	11.23	0.94	0.12
	V691	89.65	7.04	0.92	0.07
	V709	20.91	0.97	0.21	0.01
	V709	43.92	1.75	0.45	0.02
	V743	112.20	8.38	1.15	0.09
	V754	107.80	3.57	1.11	0.04
	V754	94.86	3.85	0.97	0.04
	L468	36.05	2.35	0.37	0.02
	L468	30.18	1.17	0.31	0.01
	L481	55.13	4.37	0.57	0.04
	L481	53.18	2.65	0.55	0.03
	L483	46.64	2.95	0.48	0.03
	L483	50.81	1.58	0.52	0.02
	L487	65.60	3.86	0.67	0.04
	L487	51.79	2.93	0.53	0.03

wild-type	L519	74.62	3.07	0.77	0.03
	L531	105.20	4.08	1.08	0.04
	L551	96.23	3.03	0.99	0.03
	L551	90.61	2.05	0.93	0.02
	L560	88.27	6.56	0.91	0.07
	L576	84.85	6.33	0.87	0.06
	L576	101.10	2.70	1.04	0.03
	L603	96.98	4.25	1.00	0.04
	L617	110.40	9.65	1.13	0.10
	L627	79.33	4.08	0.81	0.04
	L633	99.25	2.95	1.02	0.03
	L647	36.24	1.97	0.37	0.02
	L647	25.80	1.76	0.26	0.02
	L665	40.15	1.20	0.41	0.01
	L675	37.25	2.44	0.38	0.03
	L675	30.47	2.75	0.31	0.03
	L712	66.71	4.87	0.68	0.05
	L633	63.89	5.07	0.66	0.05
	L692	82.24	4.94	0.84	0.05
	L699	32.99	2.39	0.34	0.02
	L715	55.40	2.36	0.57	0.02
	L715	63.57	3.84	0.65	0.04
	L716	75.00	4.48	0.77	0.05
	L732	70.73	2.61	0.73	0.03
	L732	58.93	3.11	0.61	0.03
	L757	101.20	4.67	1.04	0.05
	L761	48.14	2.00	0.49	0.02
	L763	34.90	0.71	0.36	0.01
E565A	I503	30.37	3.47	0.31	0.04
	I541	26.42	1.75	0.27	0.02
	I547	87.43	5.80	0.90	0.06
	I548	89.70	8.10	0.92	0.08
	I563	74.02	7.81	0.76	0.08
	I590	25.10	1.19	0.26	0.01
	I623	51.20	3.41	0.53	0.04
	I651	26.03	1.63	0.27	0.02
	I654	31.01	2.57	0.32	0.03
	I696	82.91	8.00	0.85	0.08
	I707	28.87	2.86	0.30	0.03
	I760	76.56	3.92	0.79	0.04
	V463	12.19	0.52	0.13	0.01
	V495	63.74	4.31	0.65	0.04
	V496	50.62	2.45	0.52	0.03
	V512	57.17	4.96	0.59	0.05
	V514	84.75	16.44	0.87	0.17
	V514	91.61	11.10	0.94	0.11
	V516	71.54	8.73	0.73	0.09
	V516	72.35	7.93	0.74	0.08
	V532	84.41	8.35	0.87	0.09
	V532	88.49	6.96	0.91	0.07
	V562	101.60	20.46	1.04	0.21

	V564	77.11	7.27	0.79	0.07
	V564	82.36	6.62	0.85	0.07
	V593	51.70	2.38	0.53	0.02
	V593	37.28	1.01	0.38	0.01
	V634	82.62	12.31	0.85	0.13
	V634	96.47	13.01	0.99	0.13
	V639	87.04	9.56	0.89	0.10
	V667	98.02	10.43	1.01	0.11
	V679	60.82	2.60	0.62	0.03
	V691	82.50	17.43	0.85	0.18
	V691	80.17	8.98	0.82	0.09
	V709	22.29	1.88	0.23	0.02
	V709	37.99	1.91	0.39	0.02
	V743	95.85	7.48	0.98	0.08
	V754	101.90	6.83	1.05	0.07
	V754	93.38	3.55	0.96	0.04
	L468	36.10	1.54	0.37	0.02
	L468	31.72	2.38	0.33	0.02
	L481	44.63	4.82	0.46	0.05
	L481	47.79	4.96	0.49	0.05
	L483	37.01	2.87	0.38	0.03
	L483	53.11	1.88	0.55	0.02
	L487	63.09	4.53	0.65	0.05
	L487	57.21	2.52	0.59	0.03
	L519	63.88	4.22	0.66	0.04
E565A	L531	107.90	4.96	1.11	0.05
	L551	68.59	4.68	0.70	0.05
	L551	67.28	3.55	0.69	0.04
	L560	82.82	7.52	0.85	0.08
	L576	82.57	9.31	0.85	0.10
	L576	103.20	5.92	1.06	0.06
	L603	87.70	7.05	0.90	0.07
	L617	74.99	11.32	0.77	0.12
	L627	77.72	9.92	0.80	0.10
	L633	88.73	8.61	0.91	0.09
	L647	38.11	2.73	0.39	0.03
	L647	37.20	4.30	0.38	0.04
	L665	47.07	2.79	0.48	0.03
	L675	35.02	2.16	0.36	0.02
	L675	28.31	1.84	0.29	0.02
	L712	60.56	4.81	0.62	0.05
	L633	53.40	6.19	0.55	0.06
	L692	77.14	7.91	0.79	0.08
	L699	31.77	1.89	0.33	0.02
	L715	53.32	5.03	0.55	0.05
	L715	52.63	3.57	0.54	0.04
	L716	62.77	5.51	0.64	0.06
	L732	78.26	3.07	0.80	0.03
	L732	57.15	6.43	0.59	0.07
	L757	109.20	5.03	1.12	0.05
	L761	51.78	5.95	0.53	0.06
	L763	34.80	1.62	0.36	0.02

Table S3. Supplemental table related to Figure 4. Bioinformatic analysis of tyrosine kinases used to derive a general activation mechanism involving the molecular brake.

Kinase	Molecular Brake[a]	PDB ID	Residue at 547 position	Residue at 645 position	"I547" chi1 (deg)	"F645" chi1 (deg)	"I547-K641" distance (Å)[b]
ALK	REK	2yjs	I1179	F1271	-64.5	-70.0	5.0
ALK	REK	4anl	I1179	F1271	-66.4	-67.5	4.9
ALK	REK	4fnw	I1179	F1271	-67.1	-70.8	5.0
ALK	REK	2yjr	I1179	F1271	-63.5	-65.1	5.1
ALK	REK	4fnx	I1179	F1271	-65.1	-65.6	5.1
ALK	REK	2yhv	I1179	F1271	-63.2	-71.0	5.1
ALK	REK	3lct	I1179	F1271	-57.4	-68.6	5.2
ALK	REK	3l9p	I1179	F1271	-65.7	-68.8	5.0
EPHA2	REK	4p2k	I675	F758	-62.6	-74.2	5.1
EPHA2	REK	4trl	I675	F758	-64.3	-60.6	5.0
EPHA2	REK	1mqb (1)	I675	F758	-59.9	-53.4	4.7
EPHA2	REK	1mqb (2)	I675	F758	-58.4	-67.0	4.4
EPHA3	REK	2qoi	I682	F765	-54.2	-66.7	5.2
EPHA3	REK	2qof	I682	F765	-55.6	-65.7	5.2
EPHA3	REK	2qod	I682	F765	-58.2	-67.5	5.3
EPHA3	REK	2qol	I682	F765	-55.0	-68.7	5.2
EPHA3	REK	2qoo	I682	F765	-53.1	-63.7	5.3
EPHA3	REK	2qoc	I682	F765	-59.6	-62.9	5.2
EPHA3	REK	2gsf	I682	F765	-66.2	-66.9	5.2
EPHA3	REK	2qo7	I682	F765	-57.5	-62.4	5.1
EPHA8	REK	3kul (1)	I696	F779	-55.8	-63.8	4.8
EPHA8	REK	3kul (2)	I696	F779	-55.9	-61.3	5.0
EPHB1	REK	3zfx (1)	I680	F763	-61.7	-62.1	4.8
EPHB1	REK	3zfx (2)	I680	F763	-58.1	-62.1	4.7
EPHB1	REK	3zfx (3)	I680	F763	-58.6	-66.1	4.8
EPHB1	REK	3zfx (4)	I680	F763	-64.6	-63.9	5.0
EPHB1	REK	3zfx (5)	I680	F763	-61.6	-63.4	4.8
EPHB1	REK	3zfx (6)	I680	F763	-63.4	-61.1	4.9
EPHB1	REK	3zfx (7)	I680	F763	-61.4	-64.2	4.9
EPHB1	REK	3zfx (8)	I680	F763	-68.0	-62.7	5.2
EPHB1	REK	3zfx (9)	I680	F763	-61.3	-64.6	4.6
SYK	REK	4fl1	I432	F513	-66.3	-73.0	4.2
SYK	REK	1xba	I432	F513	-62.4	-70.7	3.9
SYK	REK	4xg2	I432	F513	-63.5	-69.4	3.8

ZAP70	REK	4k2r	I398	F480	66.1	31.3	3.1
FAK1	KEK	2ijm (1)	I483	F565	-69.5	-51.1	5.2
FAK1	KEK	2ijm (2)	I483	F565	-68	-76.2	5.0
FAK2	KEK	3cc6	I486	F568	-56.0	-75.5	4.6
FAK2	KEK	3fzo	I486	F568	-56.4	-81.9	4.3
FGFR1	NEK	4rwi (1)	I544	F642	68.1	54.3	3.0
FGFR1	NEK	4rwi (2)	I544	F642	69.5	57.5	3.2
FGFR1	NEK	3kxx (1)	I544	F642	-70.3	-63.8	4.1
FGFR1	NEK	3kxx (2)	I544	F642	-61.9	-66.2	3.6
FGFR1	NEK	3kxx (3)	I544	F642	52.3	-63.7	3.5
FGFR1	NEK	3kxx (4)	I544	F642	67.9	-65.9	3.4
FGFR1	NEK	5flf (1)	I544	F642	-62.5	-72.5	3.7
FGFR1	NEK	5flf (2)	I544	F642	-66.8	-75.9	4.4
FGFR1	NEK	5flf (3)	I544	F642	-53.1	-70.1	3.7
FGFR1	NEK	5flf (4)	I544	F642	-68.3	-71.1	3.6
FGFR1	NEK	5flf (5)	I544	F642	63.5	46.9	3.3
FGFR1	NEK	4uwy (1)	I544	F642	67.4	54.1	3.2
FGFR1	NEK	4uwy (2)	I544	F642	66.8	53.8	3.3
FGFR1	NEK	3ky2 (1)	I544	F642	62.4	57.0	3.5
FGFR1	NEK	3ky2 (2)	I544	F642	59.3	55.6	3.3
FGFR1	NEK	1fgk (1)	I544	F642	74.7	57.8	3.1
FGFR1	NEK	1fgk (2)	I544	F642	68.5	56.5	3.2
FGFR1	NEK	3gqi	I544	F642	-80.4	-71.6	4.7
FGFR2	NEK	2pvf	I547	F645	-68.4	-68.9	4.6
FGFR2	NEK	2q0b (1)	I547	F645	-67.9	-74.6	4.1
FGFR2	NEK	2q0b (2)	I547	F645	-73.4	-63.3	3.3
FGFR2	NEK	4j95 (1)	I547	F645	69.6	-67.7	3.6
FGFR2	NEK	4j95 (2)	I547	F645	-81.8	-69.8	3.4
FGFR2	NEK	4j95 (3)	I547	F645	81.6	-70.6	3.7
FGFR2	NEK	4j95 (4)	I547	F645	-83.1	-70.5	3.7
FGFR2	NEK	4j97 (1)	I547	F645	-64.9	-69.4	5.0
FGFR2	NEK	4j97 (2)	I547	F645	-65.3	-66.3	5.1
FGFR2	NEK	4j97 (3)	I547	F645	-69.0	-65.8	4.3
FGFR2	NEK	4j97 (4)	I547	F645	-80.3	-68.3	5.1
FGFR2	NEK	4j96 (1)	I547	F645	-73.3	-74.9	3.3
FGFR2	NEK	4j96 (2)	I547	F645	-70.2	-76.3	4.2
FGFR2	NEK	2pzp (1)	I547	F645	-68.8	-71.2	4.4
FGFR2	NEK	2pzp (2)	I547	F645	-66.6	-71.5	3.9
FGFR2	NEK	2pwl (1)	I547	F645	-74.2	-67.0	4.1
FGFR2	NEK	2pwl (2)	I547	F645	-66.1	-66.4	4.2

FGFR2	NEK	4j98 (1)	I547	F645	-80.1	-74.7	3.2
FGFR2	NEK	4j98 (2)	I547	F645	-79.6	-74.9	3.8
FGFR2	NEK	2pvy (1)	I547	F645	-78.3	-66.2	4.8
FGFR2	NEK	2pvy (2)	I547	F645	-76.6	-66.2	5.2
FGFR2	NEK	2pvy (3)	I547	F645	-74.3	-66.7	4.1
FGFR2	NEK	2pvy (4)	I547	F645	-76.2	-66.5	4.7
FGFR2	NEK	2pz5 (1)	I547	F645	-69.4	-71.7	4.3
FGFR2	NEK	2pz5 (2)	I547	F645	-72.2	-70.9	4.2
FGFR2	NEK	4j99 (1)	I547	F645	77.9	-68.2	3.4
FGFR2	NEK	4j99 (2)	I547	F645	74.9	-69.0	4.2
FGFR2	NEK	4j99 (3)	I547	F645	-66.9	-68.3	3.2
FGFR2	NEK	4j99 (4)	I547	F645	78.5	-67.2	3.2
FGFR2	NEK	3b2t (1)	I547	F645	-65.8	-63.9	4.4
FGFR2	NEK	3b2t (2)	I547	F645	-61.6	-62.9	4.1
FGFR2	NEK	3cly	I1547	F1645	-64.8	-69.5	5.1
FGFR2	NEK	2py3 (1)	I547	F645	-74.6	-72.0	5.2
FGFR2	NEK	2py3 (2)	I547	F645	-73.9	-72.2	4.3
FGFR2	NEK	2psq (1)	I547	F645	-75.9	-61.0	3.2
FGFR2	NEK	2psq (2)	I547	F645	-75.8	-64.1	2.5
FGFR3	NEK	4k33	I538	F636	-71.2	-68.2	4.9
FGFR4	NEK	4qqj	I533	F631	72.5	51.7	3.1
FGFR4	NEK	4tyg	I533	F631	70.9	55.8	4.0
FGFR4	NEK	4qqt	I533	F631	71.6	51.7	3.1
FGFR4	NEK	4tye	I533	F631	65.5	74.7	3.8
KIT	NEK	1pkg (1)	I653	F811	-86.4	-69.8	5.2
KIT	NEK	1pkg (2)	I653	F811	-46.4	-69.1	4.0
EPHA5	HEK	2r2p	I736	F819	-72.7	-52.0	5.1

[a] Three residues comprising the molecular brake of the respective kinase. The sites correspond to the analogous positions of N549, E565, and K641 within FGFR2K.

[b] The I547-K641 distance is between the side chain nitrogen of the lysine and the backbone carbonyl oxygen of the isoleucine. In FGFR2K numbering, these residues correspond to I547 and K641.